

## Supporting Information

### An electrostatic duel: subtle differences in catalytic performance of monoamine oxidase A and B isoenzymes elucidated at a residue level by quantum computations

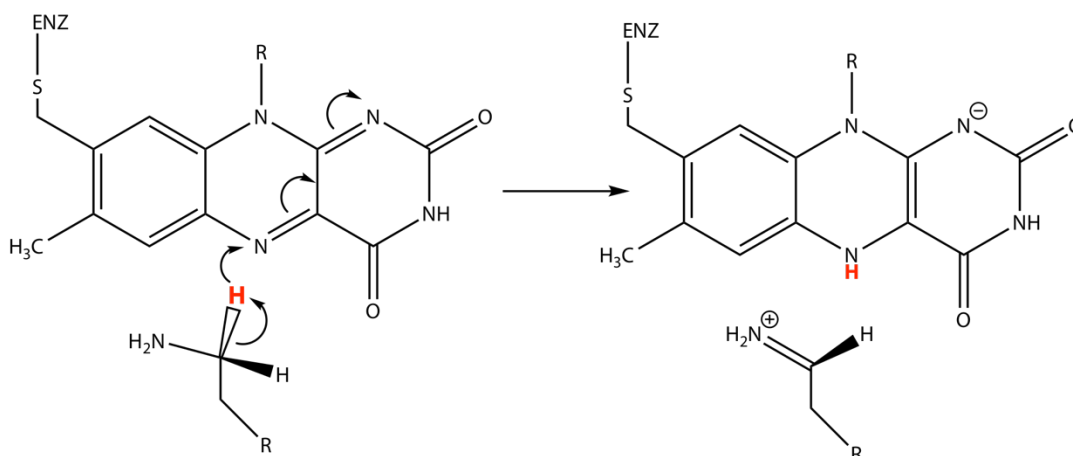
Alja Prah,<sup>†,‡</sup> Janez Mavri<sup>†</sup> and Jernej Stare<sup>\*,†</sup>

<sup>†</sup>Theory Department, National Institute of Chemistry, 1001 Ljubljana, Slovenia

<sup>‡</sup>Faculty of Pharmacy, University of Ljubljana, 1000 Ljubljana, Slovenia

\*jernej.stare@ki.si

**S1. Scheme of the rate-limiting step for the reaction between phenylethylamine (PEA) and the truncated monoamine oxidase (MAO) cofactor, lumiflavin (LFN).** The reaction was modeled based on the presumed hydride transfer mechanism. More details about the reaction and its mechanism can be found in our previous work.<sup>1-4</sup>



#### S2. Details on simulation of reactions.

Representative geometries of our system were derived from preceding molecular dynamics simulations of the rate-limiting step of PEA oxidation by the monoamine oxidase enzyme. For the MAO A isoenzyme, the simulation details were published in our previous work.<sup>2</sup> The simulations were based on crystallographic structures of both MAO enzymes, deposited in the Protein Data Bank (ID code 2Z5X for MAO A and 1GOS for MAO B). We used the OPLS-AA force field<sup>5-7</sup> for the description of our system, which was enclosed by a spherical simulation cell (30 Å radius, centered on the reacting N atom of the flavin cofactor), encompassing the enzyme with a manually docked PEA molecule and roughly 1900 water molecules. Both systems were primarily relaxed in 10 distinctive steps, where the temperature was slowly raised from 1 K to 300 K, the timestep was gradually increased from 0.1 fs to 1 fs and the restraints on the reactive subsystem were slowly relaxed. It is important to note that special care was taken in order to dock the PEA molecule as similarly as possible into both active sites (i.e., achieve a similar relative position of PEA to the flavin cofactor), so as to minimize the variation between the isoenzymes.

The simulation of the reaction was based on the Free Energy Perturbation/Umbrella Sampling approach,<sup>8-9</sup> along with the Empirical Valence Bond (EVB) protocol<sup>10-12</sup> in order to calculate the

pertinent free energy profiles. The force field of the reactants was linearly transformed into the force field of the products in 51 steps *via* the following equation:

$$H(\lambda) = \lambda \cdot H_R + (1 - \lambda) \cdot H_P,$$

where the coupling parameter  $\lambda$  was varied from 1 (reactants) to 0 (products). For both isoenzymes, 10 independent replicas were generated, all with 51  $\lambda$ -steps of 10 ps. The EVB methodology was used to generate free energy profiles and calculate the average free energy barrier for both isoenzymes. As is common with the EVB protocol, the free energy profiles for the reaction in the enzyme were generated by using parameters derived from gas phase simulations of the reaction between PEA and LFN, described in our previous work.<sup>13</sup>

The calculated difference of 1.27 kcal/mol between the barriers of both isoenzymes was in excellent agreement with the experimentally determined difference of 1.28 kcal/mol. All simulations and free-energy calculations were performed with the Q5 software package.<sup>14</sup>

Structures of our system corresponding to the state of reactants and the transition state were identified from the free energy profiles and extracted from the molecular dynamics trajectories.

### S3. Details on evaluation of the effect of electrostatic environment.

The first value we calculated was the energy barrier difference, which is determined by the following equation:

$$\Delta E = E_{OFF} - E_{ON} = (\langle E_{OFF}^{TS} \rangle_{snapshots} - \langle E_{OFF}^R \rangle_{snapshots}) - (\langle E_{ON}^{TS} \rangle_{snapshots} - \langle E_{ON}^R \rangle_{snapshots}),$$

where  $E_{OFF}$  is the energy difference between the transition state (TS) and the state of reactants (R) when the charges are turned "OFF" (i.e., not present) and  $E_{ON}$  is the energy difference between the transition state (TS) and the state of reactants (R) when the charges are turned "ON" (i.e., present). All values were averaged over 100 snapshots.

For both isoenzymes, the inclusion of the electrostatic environment (charges "ON") results in a lower energy barrier compared to the state with charges "OFF". This barrier lowering effect amounts to 14.22 kcal/mol in the MAO A enzyme and 17.54 kcal/mol in MAO B, which means that the inclusion of the electrostatic environment lowers the barrier by 3.32 kcal/mol more in the MAO B isoenzyme. This is in fairly good agreement with the experimental values reported, where the free energy barrier for this reaction is 1.28 kcal/mol lower in the MAO B isoenzyme than in MAO A.<sup>15</sup>

In a similar manner to the calculated energy barrier difference, the influence of the electrostatic environment on the charge transfer between the two reacting moieties during the transition from R to TS was determined using the Natural Bond Orbital method. The charge transfer is defined as the difference between the sum of the atomic charges of all PEA atoms in the transition state and in the reactant state. The value given in Table 1 represents the increase in charge transfer when the electrostatic environment is included – i.e., in the state with the charges ON the amount of charge transferred is increased in both isoenzymes by 0.156 and 0.184 a. u., respectively. As mentioned above, the presumed mechanism of this rate-limiting step is hydride transfer from PEA to LFN, which means that negative charge is transferred from PEA to LFN. Therefore, an increase in the amount of charge transferred reflects an enhancement of the reaction due to the presence of the electrostatic environment. As evident with the energy barrier and in agreement with the experimental data, this increase in charge transfer when the electrostatic environment is included is more pronounced in the isoenzyme MAO B than in isoenzyme MAO A (by about 0.03 charge units).

Consistent with the increased charge transfer, the difference in dipole moments of TS and R of the reacting moiety also increases upon inclusion of the electrostatic environment in both isoenzymes. Again, this increase is more pronounced in the MAO B isoenzyme compared to the MAO A isoenzyme by about 0.4 D.

Next, we considered the HOMO-LUMO gap between the two frontier molecular orbitals relevant to this reaction, i.e., the HOMO of PEA and the LUMO of LFN. A narrower HOMO-LUMO gap indicates higher reactivity between the two molecules. Again, the inclusion of the electrostatic environment (charges turned ON) in both isoenzymes causes the HOMO-LUMO gap to become narrower when going from R to TS. And in line with other parameters, this gap-narrowing effect is more pronounced (by about 23 %) in the MAO B isoenzyme.

**S4. A more detailed version of Table 1.** The experimental enzymatic free energy barrier is given for both isoenzymes. In addition, the calculated energy barriers for both enzymes and both states (charges ON and OFF) are given, as well as their differences (i.e., the barrier lowering effect of the enzymatic environment). For the charge transfer, dipole moment and HOMO-LUMO gap, the calculated values are given for both R and TS with charges turned ON or OFF in both enzymes (all values are averaged over 100 snapshots).

	MAO A				MAO B			
	ON		OFF		ON		OFF	
	R	TS	R	TS	R	TS	R	TS
$\Delta G_{exp}^\ddagger$ [kcal/mol]	<b>18.57</b>				<b>17.29</b>			
energy barrier [kcal/mol]	26.09		40.31		19.71		37.25	
	<b>14.22</b>				<b>17.54</b>			
charge transfer [a. u.]	0.0132	0.5617	0.0076	0.4001	0.0206	0.6109	0.0130	0.4191
	0.549		0.393		0.5903		0.4062	
	<b>0.156</b>				<b>0.184</b>			
dipole moment [D]	14.34	15.90	10.62	11.34	13.04	14.88	10.35	10.98
	1.56		0.72		1.84		0.63	
	<b>0.84</b>				<b>1.21</b>			
HOMO-LUMO gap [a. u.]	0.2037	0.1399	0.2147	0.1731	0.1988	0.1293	0.2152	0.1723
	0.0638		0.0416		0.0695		0.0429	
	<b>0.022</b>				<b>0.027</b>			

**S5. Alignment of primary sequences of MAO A and MAO B isoenzymes.** Amino acid residues marked in blue font color are positively charged, while residues marked in red are negatively charged. Green squares represent residue pairs where the MAO A residue is more catalytic, while orange squares mean the opposite. A lighter color denotes that  $|\Delta\Delta G_{elec}^{\ddagger}(x)| > 0.05$ , while a stronger color means that  $|\Delta\Delta G_{elec}^{\ddagger}(x)| > 0.1$ .

```

MAOA  --HMFdVvVvIGGGISGLSAAKLLTEYGVSVLVLEARDRVGGRTYTIIRNEHVdYVDVGGAY
MAOB  MSNKCDVvVvVGGGISGMAAAKLLHDSGLNVVvVLEARDRVGGRTYTLRNQKVKYVDLGGSY

MAOA  VGPTQNRILRLSKELGIETYKVNVSERLVQYVKGKTYPFRGAFPPVWNPIAYLDYNNLWR
MAOB  VGPTQNRILRLAKELGLIETYKVNVEVERLIHHVKGKSYPFRGPFPPVWNPIYLDHNNFWR

MAOA  TIDNMGKEIPTDAPWEAQHADKWDKMTMKELIDKICWTKTARRFAYLFVNINVTSEPHIV
MAOB  TMDDMGREIPSDAPWKAPLAEEDNMTMKELLDKLCWTESAKQLATLFVNLCVTAETHIV

MAOA  SALWFLWYVKQCGGTRIFSVTNGGQERKFVGGSGQVSEERIMDLLGDQVKNLHPVTHVDQ
MAOB  SALWFLWYVKQCGGTRIIISTTNGGQERKFVGGSGQVSEERIMDLLGDRVKLERPVIYIDQ

MAOA  SSDNII IETLNHEHYECKYVINAI PPTLTAKIHFPELPAERNQLIQRLPMGAVIKCMMY
MAOB  TRENVLVETLNHEMYEAKYVISAI PPTLGMKIHFNPPLPMMRNQMITRVPLGsvIKCIVY

MAOA  YKEAFWKKKDYCGCMIIEDEDAPISITLDDTKPDGSLPAIMGFILARKADRLAKLHKEIR
MAOB  YKEPFWRKKDYCGTMIIDGEEAPVAYTLDDTKPEGNYAAIMGFILAHKARKLARLTKEER

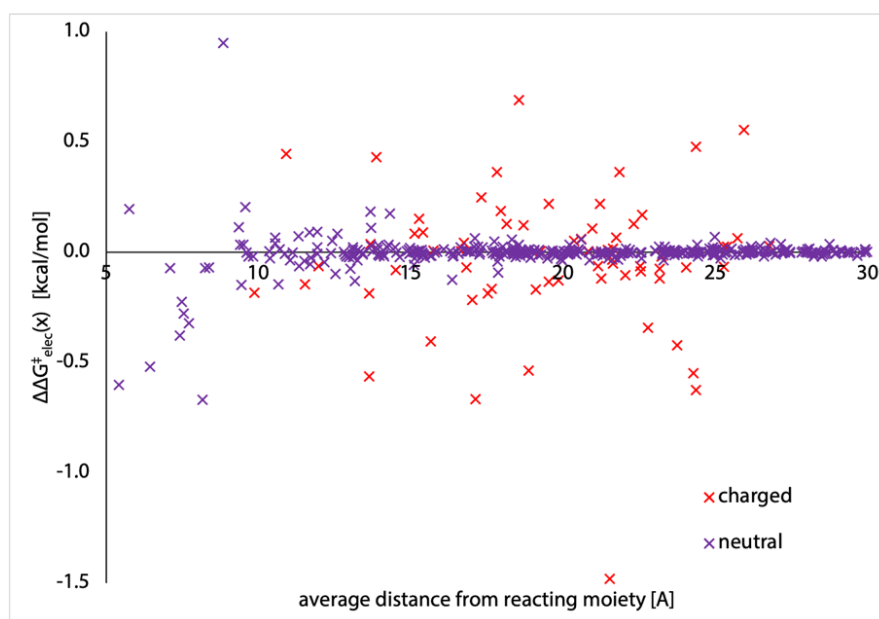
MAOA  KKKICELYAKVLGSQEALHPVHYEEKNWC EEQYSGGCYTAYFPPGIMTQYGRVIRQPVGR
MAOB  LKKLCELYAKVLGSLEALEPVHYEEKNWC EEQYSGGCYTTYFPPGILTQYGRVLRQPVDR

MAOA  IFFAGTETATKWSGYMEGAV EAGERAREVLNGLGKVTEKDIWVQEPESKDVPVEITHT
MAOB  IYFAGTETATHWSGYMEGAV EAGERAREILHAMGKIPEDEIWQSEPESDVPAQPITTT

MAOA  FWERNLPSVSGLLKIIIGFSTSV--TALGFVLYKYKLL---
MAOB  FLERHLPSVPGLLRLLIGLTTIFSATALGF LAHKRGLLVRV

```

**S6. Difference in contributions to the barrier change  $\Delta G_{elec}^{\ddagger}(x)$  (based on the interaction between the dipole moment of the reacting moiety and the electric field exerted by the enzymatic environment) between MAO A and MAO B, as a function of the average distance from the reacting moiety.** Note that a negative value indicates that the MAO B residue is more catalytic of the two, while for the positive value the opposite is true. Red crosses mark residue pairs where at least one of the two residues is charged, while violet crosses mark pairs where both residues are neutral.



**S7. List of all MAO A and MAO B residue pairs with corresponding calculated  $\Delta G_{elec}^\ddagger(x)$  values.** The name and residue number of all residues is given, as well as the average distance of the residue from the reacting moiety and its individual  $\Delta G_{elec}^\ddagger(x)$  contribution, based on the interaction between the electric field of the enzymatic environment and the dipole moment of the reacting moiety. A negative value of  $\Delta G_{elec}^\ddagger(x)$  denotes the lowering of the barrier (a catalytic effect of the residue), while the opposite is true for a positive value of  $\Delta G_{elec}^\ddagger(x)$ . Finally, the difference in  $\Delta G_{elec}^\ddagger(x)$  i.e.,  $\Delta\Delta G_{elec}^\ddagger(x)$  between the isoenzymes is calculated. A negative value in this case means that the MAO B residue provides a more significant lowering of the barrier than the corresponding MAO A residue and vice versa for the positive value. Entries are sorted by  $\Delta\Delta G_{elec}^\ddagger(x)$ . The red lines are drawn at  $\pm 0.1$  kcal/mol.

res name MAO A	res ID MAO A	dist. MAO A [Å]	$\Delta G_{elec}^\ddagger(x)$ MAO A [kcal/mol]	res name MAO B	res ID MAO B	dist. MAO B [Å]	$\Delta G_{elec}^\ddagger(x)$ MAO B [kcal/mol]	$\Delta\Delta G_{elec}^\ddagger(x)$ [kcal/mol]
ASN	181	8.64	-1.51	CYS	172	9.06	-0.57	0.95
ASP	359	19.24	-0.11	ARG	350	17.88	0.58	0.69
ASN	241	26.29	-0.02	GLU	232	25.60	0.54	0.55
ASH	343	24.43	-0.01	GLU	334	24.32	0.47	0.48
ASP	64	11.15	2.93	ASP	55	10.66	3.37	0.44
ASP	339	14.25	1.42	ASP	330	13.49	1.85	0.43
GLU	399	18.17	0.32	GLU	390	17.49	0.68	0.36
LYS	370	22.25	-0.39	LEU	361	21.47	-0.02	0.36
ARG	76	17.95	-0.03	ARG	67	16.66	0.21	0.25
GLU	329	20.19	-0.80	GLU	320	22.22	-0.58	0.22
GLU	228	19.95	1.06	GLU	219	19.13	1.28	0.22
MET	350	9.43	-0.35	MET	341	9.70	-0.15	0.20
GLY	67	5.90	-2.13	GLY	58	5.60	-1.94	0.20
GLU	185	17.91	-0.86	GLU	176	18.00	-0.68	0.18
TYR	53	13.72	-0.05	TYR	44	13.63	0.14	0.18
CYS	323	14.19	-0.03	THR	314	14.45	0.14	0.17
ASP	46	22.89	0.71	ASP	37	22.33	0.88	0.17
GLU	400	15.30	1.20	GLU	391	15.25	1.35	0.15
LYN	372	22.34	-0.03	LYS	363	22.29	0.10	0.13
LYS	90	18.35	-0.05	LYS	81	17.93	0.08	0.13
LYS	199	18.76	0.73	LYS	190	18.62	0.85	0.12
THR	183	9.47	0.21	THR	174	9.26	0.32	0.11
ALA	409	13.40	-0.13	THR	400	14.01	-0.02	0.11
GLU	43	21.12	0.86	GLU	34	20.80	0.97	0.11
VAL	65	11.58	-0.06	LEU	56	12.27	0.03	0.09
GLN	74	11.81	0.43	GLN	65	11.56	0.52	0.09
ARG	206	15.27	0.77	ARG	197	15.54	0.85	0.09
ARG	217	15.28	-0.22	ARG	208	14.95	-0.13	0.08
THR	336	12.19	-0.34	THR	327	12.99	-0.26	0.08
SER	223	11.76	-0.20	SER	214	10.86	-0.13	0.07
HID	488	24.01	-0.04	THR	479	25.96	0.03	0.07
LYS	316	21.46	-0.31	ARG	307	22.03	-0.24	0.07
GLY	351	10.66	0.24	GLY	342	10.45	0.31	0.07
TYR	62	17.04	-0.09	TYR	53	17.16	-0.03	0.06
ASP	232	25.92	0.49	ASP	223	25.55	0.55	0.06
GLU	453	20.71	0.27	GLU	444	20.49	0.33	0.06
THR	340	18.53	-0.02	THR	331	18.08	0.04	0.06
GLN	99	20.13	0.00	HIE	90	21.08	0.06	0.06
GLY	301	12.74	0.18	GLY	292	12.09	0.23	0.05
GLU	87	20.76	0.53	GLU	78	19.96	0.58	0.05
ASN	212	17.88	-0.08	ASN	203	17.60	-0.03	0.05
GLU	393	16.70	0.99	GLU	384	16.80	1.03	0.04
ASH	162	26.32	0.00	ASH	153	27.30	0.04	0.04
LEU	354	10.49	0.14	LEU	345	10.61	0.18	0.04
GLH	492	26.54	-0.04	GLH	483	27.78	0.00	0.04
GLU	436	13.69	-0.05	GLU	427	13.65	-0.01	0.04
GLN	418	28.88	0.00	GLN	409	28.61	0.03	0.04
VAL	303	9.77	0.06	VAL	294	9.02	0.10	0.03
VAL	48	18.61	0.01	VAL	39	18.48	0.05	0.03
THR	408	9.55	-0.08	THR	399	9.46	-0.05	0.03
GLN	474	24.80	0.00	SER	465	24.01	0.03	0.03
GLN	401	20.27	-0.03	GLN	392	20.15	0.00	0.03
ILE	333	14.37	0.01	VAL	324	14.19	0.04	0.03
GLY	49	13.91	0.12	GLY	40	13.94	0.15	0.03
THR	417	26.86	0.00	THR	408	26.09	0.03	0.03
PHE	177	13.54	-0.36	PHE	168	13.85	-0.33	0.03
GLU	458	26.81	-0.02	GLH	449	26.74	0.00	0.03
SER	345	23.53	0.02	ASN	336	23.16	0.05	0.03
ARG	457	25.61	-0.13	ARG	448	25.16	-0.10	0.03
GLU	367	25.36	0.29	GLU	358	25.19	0.31	0.03
SER	81	17.36	-0.05	ALA	72	17.07	-0.03	0.02
LEU	294	23.02	-0.01	MET	285	23.28	0.01	0.02
THR	211	17.17	-0.05	THR	202	17.00	-0.03	0.02
ASN	92	18.26	-0.05	ASN	83	17.77	-0.03	0.02
ASN	125	26.09	-0.03	ASN	116	26.25	-0.01	0.02
THR	105	24.51	0.01	SER	96	25.32	0.03	0.02
GLY	447	11.98	0.03	GLY	438	11.88	0.06	0.02
GLY	50	13.08	0.09	GLY	41	13.13	0.12	0.02
VAL	178	14.34	-0.33	VAL	169	14.64	-0.31	0.02
ALA	355	14.45	0.08	ALA	346	14.02	0.10	0.02
PRO	186	18.11	0.01	THR	177	18.61	0.03	0.02
GLN	147	31.55	-0.01	PRO	138	30.32	0.01	0.02
THR	204	16.37	-0.11	THR	195	16.90	-0.09	0.02
ASN	75	17.55	0.05	ASN	66	17.15	0.07	0.02
ASN	396	15.22	0.06	ASN	387	14.73	0.08	0.02
ASN	133	25.44	0.00	ASH	124	25.62	0.02	0.02
ARG	454	21.83	0.04	ARG	445	21.46	0.05	0.02
HID	388	28.02	-0.01	GLH	379	28.15	0.00	0.02
GLH	375	24.71	-0.02	GLH	366	25.42	0.00	0.02
LYN	136	24.77	0.01	ARN	127	24.84	0.02	0.02
ASN	57	22.08	-0.01	ASN	48	22.05	0.01	0.01
PRO	347	20.74	0.00	ALA	338	20.30	0.01	0.01
GLN	200	13.90	0.34	GLN	191	13.92	0.35	0.01
VAL	473	25.26	-0.01	GLN	464	25.23	0.01	0.01
SER	38	33.04	-0.01	ASN	29	33.82	0.00	0.01
LYN	151	30.39	0.00	GLH	142	30.10	0.01	0.01
TRP	397	10.78	0.01	TRP	388	10.61	0.03	0.01
TYR	89	16.33	0.11	TYR	80	15.85	0.13	0.01
GLY	21	18.75	0.02	GLY	12	18.12	0.03	0.01
LEU	298	18.53	0.03	VAL	289	19.24	0.05	0.01
GLY	414	25.73	0.01	GLY	405	25.28	0.02	0.01
TYR	106	25.50	-0.02	TYR	97	26.47	-0.01	0.01
GLH	290	29.80	-0.01	MET	281	30.03	0.00	0.01
TRP	166	32.33	0.00	TRP	157	32.61	0.01	0.01
ARN	493	29.79	0.00	ARN	484	30.58	0.01	0.01
ASH	123	27.61	-0.03	ASH	114	28.44	-0.02	0.01
GLH	262	33.98	-0.01	GLH	253	33.41	0.00	0.01
ASN	126	27.04	-0.04	ASN	117	27.70	-0.03	0.01
CYS	165	26.11	-0.01	CYS	156	26.30	0.00	0.01
LEU	78	15.55	0.05	LEU	69	15.18	0.06	0.01
LEU	277	19.34	-0.01	LEU	268	19.08	0.00	0.01
VAL	220	18.83	0.04	VAL	211	17.90	0.05	0.01
TYR	124	22.67	-0.07	HIE	115	24.66	-0.06	0.01
LEU	361	18.60	0.02	LEU	352	19.17	0.03	0.01
ASP	480	21.78	0.34	ASP	471	21.14	0.35	0.01
GLY	213	13.19	0.19	GLY	204	13.00	0.20	0.01
ILE	353	12.91	0.03	ILE	344	13.61	0.04	0.01
LYN	318	26.84	-0.01	LYN	309	27.77	0.00	0.01
ALA	358	15.07	0.06	ALA	349	14.78	0.07	0.01
THR	278	21.76	0.01	GLY	269	22.61	0.02	0.01
PHE	173	18.02	-0.11	LEU	164	19.20	-0.10	0.01
SER	497	31.50	0.02	SER	488	32.49	0.03	0.01
ASH	150	30.00	-0.02	GLH	141	30.42	-0.01	0.01
MET	157	18.91	0.06	MET	148	19.21	0.07	0.01
GLN	237	29.98	-0.01	ARN	228	29.86	0.00	0.01
THR	130	24.80	0.02	THR	121	25.01	0.03	0.01
GLN	293	28.32	-0.02	GLN	284	29.43	-0.01	0.01
TRP	472	24.41	0.01	TRP	463	24.00	0.01	0.01
THR	489	28.07	-0.03	THR	480	29.14	-0.02	0.01
ASN	292	28.48	0.00	ASN	283	29.80	0.01	0.01
PRO	413	23.78	0.02	PRO	404	23.22	0.02	0.01
ILE	423	20.34	0.03	LEU	414	20.04	0.04	0.01
GLN	384	29.27	0.00	LEU	375	30.88	0.01	0.01
TRP	128	19.44	-0.02	TRP	119	19.89	-0.01	0.01
LYN	239	29.02	0.01	LYN	230	28.69	0.01	0.01
PRO	299	17.83	-0.08	PRO	290	17.50	-0.07	0.01
THR	156	23.06	0.02	THR	147	22.97	0.03	0.01
PRO	412	20.64	-0.01	PRO	403	20.35	0.00	0.01
LEU	463	34.43	0.00	MET	454	34.36	0.00	0.01
ALA	120	28.75	-0.02	THR	111	29.48	-0.01	0.01
LYN	371	25.94	-0.01	LYN	362	26.32	0.00	0.01
TRP	152	25.92	-0.03	TRP	143	25.91	-0.02	0.01





res name MAO A	res ID MAO A	dist. MAO A [Å]	$\Delta G^{\ddagger}_{elec}(k)$ MAO A [kcal/mol]	res name MAO B	res ID MAO B	dist. MAO B [Å]	$\Delta G^{\ddagger}_{elec}(k)$ MAO B [kcal/mol]	$\Delta\Delta G^{\ddagger}_{elec}(k)$ [kcal/mol]
ASH	141	22.79	0.01	ASP	132	22.79	-0.34	-0.34
ALA	68	7.42	-1.01	SER	59	7.40	-1.38	-0.38
LYS	440	16.00	0.58	HIE	431	15.32	0.18	-0.40
ASH	330	23.47	0.03	GLU	321	24.01	-0.39	-0.42
TYR	444	6.51	-1.46	TYR	435	6.36	-1.98	-0.52
ARG	356	19.46	0.55	HIE	347	18.30	0.01	-0.54
HIE	59	24.19	-0.01	LYS	50	24.39	-0.56	-0.55
LYS	395	14.05	-1.10	LYS	386	13.21	-1.66	-0.56
TYR	407	5.41	-1.55	TYR	398	5.44	-2.15	-0.60
ASH	153	24.34	0.00	ASP	144	24.38	-0.62	-0.63
VAL	93	16.96	-0.01	GLU	84	17.27	-0.67	-0.67
GLN	215	8.27	-0.55	GLN	206	8.04	-1.22	-0.67
ASP	61	21.26	0.80	LYS	52	21.79	-0.68	-1.48



## References

1. Prah, A.; Frančišković, E.; Mavri, J.; Stare, J., Electrostatics as the Driving Force Behind the Catalytic Function of the Monoamine Oxidase A Enzyme Confirmed by Quantum Computations. *ACS Catal.* **2019**, *9* (2), 1231-1240.
2. Oanca, G.; Purg, M.; Mavri, J.; Shih, J. C.; Stare, J., Insights into enzyme point mutation effect by molecular simulation: phenylethylamine oxidation catalyzed by monoamine oxidase A. *PCCP* **2016**, *18* (19), 13346-13356.
3. Pregeljč, D.; Jug, U.; Mavri, J.; Stare, J., Why does the Y326I mutant of monoamine oxidase B decompose an endogenous amphetamine at a slower rate than the wild type enzyme? Reaction step elucidated by multiscale molecular simulations. *PCCP* **2018**, *20* (6), 4181-4188.
4. Vianello, R.; Repič, M.; Mavri, J., How are biogenic amines metabolized by monoamine oxidases? *Eur. J. Org. Chem.* **2012**, *36* (36), 7057-7065.
5. Jorgensen, W. L.; Maxwell, D. S.; TiradoRives, J., Development and testing of the OPLS all-atom force field on conformational energetics and properties of organic liquids. *J. Am. Chem. Soc.* **1996**, *118* (45), 11225-11236.
6. Kaminski, G. A.; Friesner, R. A.; Tirado-Rives, J.; Jorgensen, W. L., Evaluation and reparametrization of the OPLS-AA force field for proteins via comparison with accurate quantum chemical calculations on peptides. *J. Phys. Chem. B* **2001**, *105* (28), 6474-6487.
7. Robertson, M. J.; Tirado-Rives, J.; Jorgensen, W. L., Improved Peptide and Protein Torsional Energetics with the OPLS-AA Force Field. *J. Chem. Theory Comput.* **2015**, *11* (7), 3499-3509.
8. Zwanzig, R. W., High-Temperature Equation of State by a Perturbation Method. I. Nonpolar Gases. *J. Chem. Phys.* **1954**, *22* (8), 1420-1426.
9. Kollman, P., Free-Energy Calculations - Applications to Chemical and Biochemical Phenomena. *Chem. Rev.* **1993**, *93* (7), 2395-2417.
10. Aqvist, J.; Warshel, A., Simulation of Enzyme-Reactions Using Valence-Bond Force-Fields and Other Hybrid Quantum-Classical Approaches. *Chem. Rev.* **1993**, *93* (7), 2523-2544.
11. Warshel, A.; Levitt, M., Theoretical Studies of Enzymic Reactions - Dielectric, Electrostatic and Steric Stabilization of Carbonium-Ion in Reaction of Lysozyme. *J. Mol. Biol.* **1976**, *103* (2), 227-249.
12. Warshel, A.; Weiss, R. M., An Empirical Valence Bond Approach for Comparing Reactions in Solutions and in Enzymes. *J. Am. Chem. Soc.* **1980**, *102* (20), 6218-6226.
13. Stare, J., Complete sampling of an enzyme reaction pathway: a lesson from gas phase simulations. *RSC Adv.* **2017**, *7* (15), 8740-8754.
14. Marelius, J.; Kolmodin, K.; Feierberg, I.; Aqvist, J., Q: a molecular dynamics program for free energy calculations and empirical valence bond simulations in biomolecular systems. *J. Mol. Graphics Modell.* **1998**, *16* (4-6), 213-225, 261.
15. Geha, R. M.; Rebrin, I.; Chen, K.; Shih, J. C., Substrate and inhibitor specificities for human Monoamine Oxidase A and B are influenced by a single amino acid. *J. Biol. Chem.* **2001**, *276* (13), 9877-9882.